Using enhanced crow search algorithm optimization-extreme learning machine model to forecast short-term wind power

Abstract

Wind power has strong volatility and randomness that impacts the grid and reduce the voltage quality of the grid when it is connected to the grid in large scale. The power sector takes the wind abandonment measures to ensure the grid voltage stability to reduce the clean energy utilization rate. The enhanced crow search algorithm optimization-extreme learning machine (ENCSA-ELM) model is proposed to accurately forecast short-term wind power to improve the efficiency of clean energy utilization. (1) The enhanced crow search algorithm (ENCSA) is proposed and applies to short-term wind power forecast. The convergence performance test revealed that the local development and global exploration capabilities of the ENCSA were enhanced, and the test result of the proposed ENCSA algorithm outperformed other well-known nature inspired algorithms and state-of-the-art CSA variants; (2) The output and input of the forecasting models are determined by analysis of the influence wind power factors and the wind power samples in autumn, winter and spring were forecasted by the ENCSA-ELM model; and (3) The forecast results are analyzed by evaluation indexes. The simulation experiments revealed that the error interval and evaluation indexes of the ENCSA-ELM model outperformed the state-of-the-art wind power forecast models, traditional machine learning models and ELM optimized by other algorithms. The proposed model on *RMSE* value and *MAPE* value are controlled below 20% and 4%. Accurate wind power prediction has an impact on maintaining the voltage stability of power grid and increases the efficiency of clean energy utilization.

Keywords: extreme learning machine; forecasting; short-term wind power; clean energy; enhanced crow search algorithm optimization

1. Introduction

The demand for energy has increased due to the rapid growth of the world economy. The increase of fossil energy production and large consumption leads to a series of problems (Liu et al., 2020). The massive consumption of fossil energy progresses to destroy the environment, and large-scale mining accelerates the depletion of fossil energy (Dong and Shi, 2019). Clean energy is a kind of renewable energy without the possibility of exhaustion, which has an important impact on enhancing sustainable development level and improving environmental quality (Kamat, 2007). The utilization of clean energy brings inestimable ecological and economic benefits (Jacobson et al., 2011). As a kind of clean energy, wind energy has huge reserves and high commercial development value and has developed rapidly in recent years (Papadopoulos, 2020; Guermoi et al., 2018). According to the statistics of the Global Wind Energy Council (GWEC), by the end of 2014, the installed capacity of wind power in the world has reached 360GW, while the installed capacity of China is 115GW. It is estimated that by 2030 and 2050, the installed capacity exceeds 400 GW and 1000 GW to meet 8.4% and 17% of China's power demand (Wang et al., 2020).

Wind energy has strong volatility and randomness (Xia et al., 2020). Large scale wind

power integration impacts the power network operation, and result in the decline of power quality. This characteristic leads to the phenomenon of wind abandonment and reduce the utilization rate of clean energy. Accurate wind power forecasting technology provides decision support for grid connected dispatching, reduce wind abandonment measures and maintain the power quality, so it is significance to predict wind power (Vargas et al., 2019). According to different prediction intervals, wind power forecasting methods usually include medium-long-term forecast, short-term forecast and ultra-short-term forecast (Salcedo-Sanz., 2011; Foley et al., 2012). The medium- and long-term wind power forecast period is several weeks or months, which is used to formulate grid maintenance plans. The Ultra-short-term forecasting is aimed at predicting wind power within the next 4 hours and is used for solving frequency modulation problems and power grid dispatching (Ma et al., 2020; Dupre et al., 2020). The short-term forecast is for wind power within 48 hours, which is used to make the generation plan of the generator set and solve the peak shaving problem (Liu et al., 2018; Chen and Liu, 2020).

Wind power prediction methods are basically divided into three types along with different prediction models (Barbounis et al., 2006; Jung and Broadwater, 2014). The first is wind power forecast methods based on intelligent optimization algorithms and machine learning models. The second is wind power forecast method based on statistical regression models. The third is the combination methods. Statistical regression models such as autoregressive moving average model (ARMA), autoregressive model (AR) and moving average model (MA) analyze the changing law of the decomposed components by decomposing various changing components in the time series (Zhang et al., 2019; Eissa et al., 2018). Song et al., 2018 argued that most statistical regression models cannot deal with the irregular and nonlinear characteristics of wind power series due to the linear form of prior assumptions. This method is aimed at short-term wind power forecasting. With the rapid development of artificial intelligence technology, different machine learning models have been proposed to achieve high-precision forecast of wind power series with nonlinear and fluctuating characteristics (CAI et al., 2020). Common machine learning models include support vector machine (SVM) model, neural network model and relevance vector machine. (Ding et al., 2019; Diyaley et al., 2019). The key of machine learning model is to select the optimal random parameters (Chen et al., 2014).

In addition, Suresh et al. (2010) argued that the random parameters of ELM had great influence on the prediction performance of ELM model. An improved GA algorithm is proposed to optimize the random parameters of ELM to improve the prediction performance of ELM. The extreme learning machine (ELM) model is used to forecast short-term wind power. The random weights and random threshold parameters influence the wind power prediction results; hence, the random parameters problem solves by using a novel crow search algorithm (CSA). Still, the CSA algorithm itself has the problem of easily falling into a local solution. Wolpert and Macready, (1997) claimed that none algorithm can solve all optimization problems according to the theory of no free lunch and means that when the same optimization algorithm solves different problems and convergence performance is different. Developing new optimization algorithms is still necessary when dealing with different problems. The enhanced crow search algorithm (ENCSA) was proposed to obtain the optimal parameters of ELM model and improve the prediction accuracy of wind power. In the ENCSA algorithm, periodic migration strategy, adaptive flight step adjustment strategy and acceleration

coefficient were introduced. Through the above improvement measures, the ENCSA algorithm search capability was enhanced to search the random parameters. The proposed algorithm shows stronger convergence performance and obtains more satisfactory convergence results compared with well-known nature inspired algorithms and state-of-the-art CSA variants. The enhanced crow search algorithm optimization-extreme learning machine (ENCSA-ELM) model is proposed for short-term wind power forecasting. ENCSA-ELM has higher prediction accuracy, stronger generalization ability and considers the influence of seasonal factors on wind power compared with the traditional machine learning models and ELM optimized by different optimization algorithms. The objectives of this study are as follows.

- To improve the search performance of CSA algorithm;
- To solve the influence of random parameters of ELM model on the forecasting results;
- To improve the forecasting accuracy of short-term wind power.

The contributions of this study are as follows. (1) presenting the ENCSA optimization algorithm and applied it to short-term wind power forecasting; (2) searching the random parameters of the ELM model by the ENCSA algorithm and the problem that ELM model random parameters affected the prediction accuracy was addressed; (3) applying the ENCSA-ELM model for short-term wind power forecast and the propose model was verified through simulation experiments; and (4) Using accurate short-term wind power forecasting to reduce the phenomenon of wind abandonment, to promote the clean energy development and to assist the power department to formulate a reasonable dispatch plan.

The remaining sections include the following contents. Section 3 gives the basic theory of the wind power forecast model and analyzes the ENCSA algorithm. Section 4 introduces the experimental samples. Section 5 gives the assessment indicators and prediction results of short-term wind power. Section 6 introduces the important conclusions and the future study plan.

2. Literature review

This section includes the review on forecasting short-term wind power and proposed method on enhanced crow search algorithm optimization-extreme learning machine.

2.1 Forecasting short-term wind power

Short-term wind power forecasting has received extensive attention due to the importance to power systems (Shi et al., 2012). Prior studies have proposed many short-term wind power prediction methods (Catalao et al., 2011). These methods are basically divided into statistical regression models, machine learning methods and combination models (Li et al., 2020). The statistical regression models consider the time factor and does not consider other factors. The machine learning method uses machine-learning model and combines with external factors affecting wind power to forecast wind power.

The forecasting methods based on statistical regression for short-term wind power included various autoregressive models. The forecast error of linear autoregressive model is large because of the large fluctuation of wind power. Karakus et al. (2017) used polynomial autoregressive model to predict wind power. Polynomial autoregressive model belongs to nonlinear regression model, which has a good fitting effect on wind power prediction. Nonlinear regression model is more suitable for wind power prediction. Jiang et al. (2017)

combined multi-step-ahead method with statistical regression model to forecast the short-term wind power. According to the wind power curve and order determination method, Dong et al. (2011) established autoregressive moving average (ARMA) model with different orders. The forecast values were obtained by adopting the weighted average method to the ARMA models with different orders. This method improves the prediction effect to a certain extent, but the step calculation increases the running time and calculation amount. Duran et al. (2007) proposed the autoregressive model that considered exogenous variables. The model considered the time span and delay of the electricity market. Traditional linear and nonlinear AR wind power models do not consider seasonal factors. Lin et al. (2015) took seasonal variables into the wind power forecasting model. The wind power was forecasted by the nonlinear AR model, and the unknown parameters were identified by the random forest method. Both linear statistical model and nonlinear statistical model merely consider the time series when forecasting wind power, and do not involve the external factors; therefore, whilst the amount of data increases and the prediction error of the model becomes larger.

Since the time series model only considers the time factor. When the external factors change greatly, the forecast result of the model is affected (Li et al., 2018). Many studies preferred machine learning models and combinatorial models (Liu et al., 2018; Li et al., 2020). The support vector machine (SVM) is applied to the field of short-term wind power forecast due to its strong mapping ability (Habib et al., 2020). SVM also has the problem of random parameters (Fu et al., 2019). To reduce the influence of super parameters, Li et al. (2020) and Li et al. (2018) used the cuckoo search algorithm and dragonfly search algorithm to select the random parameter. Yuan et al. (2015) compared the wind power forecast effects of the least squares SVM model with different kernel functions. The parameters of the optimal kernel function were determined by optimization algorithm. SVM model is suitable for small samples, and is difficult to train large-scale data, so it is generally used for short-term and ultra-short-term wind power prediction. Zhang et al. (2020) proposed a hybrid model and used variable mode decision to decompose wind power data. The decomposed linear and nonlinear series were forecasted by the ARMA model and radial basis function network. Yin et al. (2019) proposed a multi-layer decomposition method. The original sequence was decomposed by the empirical mode decomposition method. Variable mode decision method was used to further decompose the first subsequence. The features between each factor and wind power were extracted by the convolution neural network. Finally, the predicted subsequence was superposed to get the final wind power. Although the combination of machine learning model and sequence decomposition model has better prediction effect, sequence decomposition and sequence reconstruction can increase the computational cost.

2.1 Enhanced crow search algorithm optimization-extreme learning machine

Filtering technology and neural network model are used to predict wind power. Zheng and Wu (2019) used clustering method to classify wind power samples of similar weather. The characteristic quantity which had little influence on wind power was eliminated. The short-term wind power was forecasted based on the extreme gradient boosting. Clustering algorithms are generally sensitive to noise signals. When the noise signal in wind power is large, the clustering effect has greatly affected. Cassola and burlando (2012) applied Kalman filter to wind power prediction. Kalman filter combined prediction values with observation values to

reduce the prediction error. Kalman filter is applicable to linear, discrete and finite-dimensional systems. Wind power has strong nonlinearity, so Kalman filter is usually not used to predict wind power. Liu et al. (2019) used wave transformation method to deal with the non-stationary problem of wind power. The nonlinear wind power was decomposed by wave transformation. Each decomposed sequence was forecasted by the long short term memory network model.

This kind of forecasting method based on decomposition sequence reduces the non-stationary of wind power to a certain extent, which makes the model complex and increases the calculation cost at the same time. Zhang et al. (2020) processed the heterogeneous data of wind power to improve the forecasting effect. The wind power was predicted by the back-propagation neural network (BPNN) model. Genetic algorithm was used to select random parameters of BPNN. Korprasertsak and leephakpreeda (2019) compared the forecast effects of the artificial neural network model, grey model and ARMA model. These three models were used to forecast wind power at different time stages. The three models were combined with the change of wind power over time and the result showed the smallest root mean square error.

This study is found that statistical regression model only considers time factor; SVM model is limited by samples; filtering technology is rarely used for wind power prediction due to its own limitations; although the combined model can improve the prediction results to a certain extent, the calculation cost is also greatly increased. This study proposes ENCSA-ELM model to predict wind power, and used ENCSA algorithm to solve the influence of random parameters on ELM model. The effectiveness and superiority of ENCSA algorithm and ENCSA-ELM model were verified by simulation experiments. Compared with the statistical regression model, the ENCSA-ELM model not only considers the external factors affecting wind power, but also considers the influence of seasonal factors on wind power. Compared with SVM model, the proposed model is applied not only to short-term wind power forecasting, but also to long-term wind power forecasting, with stronger generalization ability. Compared with the combination model based on sequence decomposition, ENCSA-ELM model has more advantages than the combination model based on sequence decomposition. Through the simulation test of ENCSA-ELM model, the EN_{MAPE} of ENCSA-ELM model was controlled within 4% and EN_R^2 was more than 90% in different seasons.

3. Prediction model principles

3.1 Extreme learning machine theory

The feed-forward neural network uses gradient descent to train the network. The gradient descent method has certain limitations. Many parameter values need to be set in the training process. The weights of the network need to be adjusted during the iteration process, which makes the calculation speed of the model slower. These problems limit the model development. To solve these defects, the ELM model is presented. The learning speed of the ELM model is fast since the ELM model has only one hidden layer (Huang et al., 2012; Tang et al., 2016). The ELM model has been used in various fields, such as wind speed forecasting, fault diagnosis and life prediction.

Figure 1 presents the topology of the ELM model. The ELM model includes three layers: output layer, hidden layer and input layer. Based on the back propagation method, the feed-forward neural network updates the weights during the iterative process. The ELM model has

random initial weights that does not need to be updated during the iteration process (Huang et al., 2011).

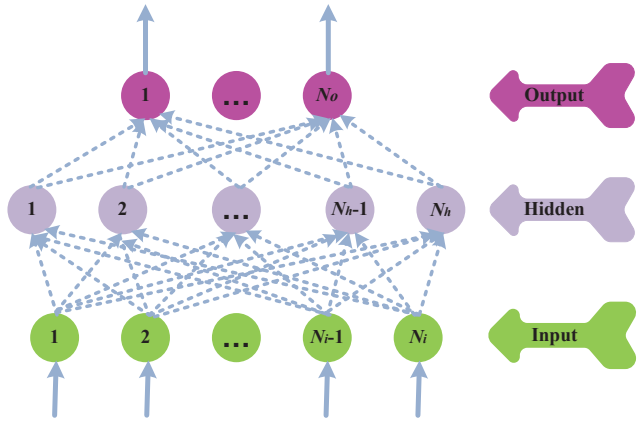

Figure 1. ELM model network structure

Assume that $T=\{(c_i, e_i)|c_i \in R^n, e_i \in R^n\}$ is the given training samples, $F(\cdot)$ is the activation function. The ELM model is expressed as equation (2) (Choudhary and Shukla. 2021; Nizar et al., 2008):

$$\begin{aligned} &\sum_{i=1}^{N_h} \alpha_i F(\rho_i c_1 + \theta_i) = e_1 \\ &\sum_{i=1}^{N_h} \alpha_i F(\rho_i c_2 + \theta_i) = e_2 \\ &\vdots \\ &\sum_{i=1}^{N_h} \alpha_i F(\rho_i c_{N_s} + \theta_i) = e_{N_s} \end{aligned} \tag{1}$$

where θ_i represents the threshold of the hidden layer node; α_i represents the weight that connects the output and the hidden layer nodes; ρ_i is the weight that connects the input and the hidden layer nodes; c_i represents the input sample of the model; e_i is the output sample of the model; N_s represents the number of samples.

The above equation is expressed as follows:

$$\boldsymbol{Y}\alpha = \boldsymbol{e} \tag{2}$$

$$\boldsymbol{Y} = \begin{bmatrix} F(\rho_1 c_1 + \theta_1) & \cdots & F(\rho_{N_h} c_1 + \theta_{N_h}) \\ \vdots & \ddots & \vdots \\ F(\rho_1 c_{N_s} + \theta_1) & \cdots & F(\rho_{N_h} c_{N_s} + \theta_{N_h}) \end{bmatrix} \tag{3}$$

$$\boldsymbol{\alpha} = [\alpha_1, \cdots, \alpha_{N_h}]^T \tag{4}$$

$$\boldsymbol{e} = [e_1, \cdots, e_{N_s}]^T \tag{5}$$

where $\boldsymbol{e}$ represents the sample label matrix; $\boldsymbol{Y}$ represents the hidden layer output matrix; α represents the weight matrix; N_h is the number of nodes in the hidden layer.

The input weight and hidden layer threshold of the ELM model are randomly determined. There is no need to adjust in the iterative process, only the output weight needs to be calculated. The output weight matrix of the ELM model is as follows:

$$\boldsymbol{\alpha} = (\boldsymbol{Y}^T \boldsymbol{Y})^{-1} \boldsymbol{Y}^T \boldsymbol{e} \tag{6}$$

The ELM prediction model is obtained.

$$e = \sum_{i=1}^{N_h} \alpha_i F(\rho_i c + \theta_i) \tag{7}$$

The specific calculation process of ELM model is shown below:

(1) Determine the sample of the model.
(2) Randomly initialize hidden layer thresholds and input weights.
(3) Calculate the output matrix.
(4) Solve the output weight of hidden layer.

3.2 Crow search algorithm principle

In nature, crow is an intelligent bird. The ratio of crow's brain volume to body is the largest among birds. The brain capacity is larger and the birds are smarter. This is more adaptable to nature. In nature, crows make tools and use them to find food. The crow search algorithm (CSA) imitates two behaviors of crow: hiding food and recalling the location of the food (askarzadeh, 2016; sayed et al., 2019). The CSA algorithm follows the following rules.

(1) Crows survive in groups.
(2) The crow hides its food and recall the location of the food.
(3) There is competition among crows. Crows steal food from each other.
(4) The crow avoids theft of food by leading competitors to other locations.

The CSA algorithm is developed based on the above rules. Suppose there are M crows in the group. The position vector of the j_{th} crow in the group is $\boldsymbol{Pos}_j^{iter}$($i$=1,2,…,$M$;$iter$=1,2,…,$Miter$). Where $Miter$ is the maximum number of iterations. $\boldsymbol{Pos}_j^{iter}$=[$\boldsymbol{pos}_{j,1}^{iter}$,…, $\boldsymbol{pos}_{j,\mathrm{dim}}^{iter}$]. dim is the dimension of the variable (Oliva et al., 2017). In the process of hiding food, each crow has an optimal position.

In the CSA algorithm, crows obtain better food positions by searching or tracking other crows. This behavior of crows is described by the perception probability (Awp_j^{iter}) and is divided into the following two situations (Gupta et al., 2018).

Case 1: Crow i did not find the tracking behavior of crow j. Then crow j finds the hiding place of crow i. In the iterative process of CSA algorithm, the position of crow is represented by m_j^{iter}. For case 1, the updated location of crow j is shown below:

$$\boldsymbol{Pos}_j^{iter+1} = \boldsymbol{Pos}_j^{iter} + R \times FL_j^{iter} \times (m_j^{iter} - \boldsymbol{Pos}_j^{iter}) \tag{8}$$

where R is a random value between 0 and 1; FL_j^{iter} represents the flying distance of crow during the iteration. The flight distance determines the length of the crow's flight to the food storage location. When the flying distance is large, the crow has a strong global search ability; when the flying distance is small, the crow has a strong local exploitation ability.

Case 2: when crow i finds the tracking behavior of crow j, crow i leads crow j to a random position to avoid stealing his food.

According to the description of case 1 and case 2, the location update method of crow j is shown in equation 9:

$$\begin{cases} \boldsymbol{Pos}_j^{iter+1} = \boldsymbol{Pos}_j^{iter} + R \times FL_j^{iter} \times (m_j^{iter} - \boldsymbol{Pos}_j^{iter}) & R \geq Awp_j^{iter} \\ \boldsymbol{Pos}_j^{iter+1} = \boldsymbol{Pos}_{rand} & R < Awp_j^{iter} \end{cases} \tag{9}$$

In the CSA algorithm, the search ability is changed by controlling Awp. When Awp is small, crows search by themselves. So the crow has a strong local development capability. When Awp is large, crows are led to random positions. The crow has a strong global search capability.

3.3 Enhanced crow search algorithm principles

The CSA algorithm itself has certain limitations to reflect in the following two aspects. (1) The flight step size in the CSA algorithm is a fixed value and does not change with the number of iterations, which limits the crow's global search and local exploitation capabilities. (2) The crow population diversity is adjusted by *Awp* in the CSA algorithm. *Awp* is a certain value to limit the coordination ability of the algorithm during the iterative process.

In view of the CSA algorithm limitations, this study proposes the ENCSA based on flight migration strategy and adaptive flight step adjustment strategy. Through the regular flight migration strategy, the crow population is prevented from the problem of population simplification in the later iteration. The ENCSA algorithm enhances the ability of crow's global exploration and local development through adaptive flight step adjustment strategy. So the convergence speed of the algorithm is accelerated.

A. Regular flight migration strategy

The diversity of crow population is maintained by setting migration frequency (MF). At the beginning of iteration, judge whether crows need to migrate. If crows need to migrate and flies to other places to search. If crows don't need to migrate and searches by themselves or follow other crows. The location updating equation of the crow after migration is as follows:

$$\begin{cases} \boldsymbol{Pos}_j^{iter+1} = \boldsymbol{Pos}_j^{iter} + R \times L \times (m_{best} - \boldsymbol{Pos}_j^{iter}) \\ L = e^{\frac{f_j - f_{best}}{f_j + \varepsilon}} \end{cases} \tag{10}$$

where R represents the random number of [0, 1] interval; m_{best} represents the optimal crow position in crow group; f_j represents the target value of crow j; f_{best} represents the target value of the optimal individual; ε represents the infinitesimal, which ensures that the fraction is meaningful.

The migration formula of the crow group found that the crow group does not migrate to a random position, but follows the crow with the best position in the group. The migration of crows is not blind, so as to speed up the convergence of crows.

B. Adaptive flight step adjustment strategy

In the CSA algorithm, the flight distance is a fixed value. The search ability of the crow cannot be adjusted with the increase of iteration. An adaptive flight step size is proposed. When the number of iterations increases, the search ability of crows is adjusted. The mathematical model of adaptive flight step is as follows:

$$FL_j^{iter} = 0.2 \times e^{\frac{Miter}{iter}} \tag{11}$$

With the deepening of the crow search, the flight step size gradually becomes smaller. In the initial stage of optimization, the crow has a larger flight step size, which makes the crow have a strong global search capability. At the end of the iteration, the flight step size of the crow becomes smaller, which makes the crow strengthen the local development capability.

C. Acceleration search factor

The adaptive search step can strengthen the crow's global search and local development capabilities. The acceleration search coefficient (ASC) is introduced to further improve the crow's optimization capability. The mathematical model of ASC is shown in equation (12).

$$ASC = ASC_{\min} + (ASC_{\max} - ASC_{\min}) \times e^{(-15 \times \frac{iter}{Miter})^5} \tag{12}$$

where $ASC_{\max}$($ASC_{\max}$=0.9) and $ASC_{\min}$($ASC_{\min}$=0.2) are the maximum and minimum values.

Figure 2 depicts the variation curve of *ASC* changing with evolving algebra.

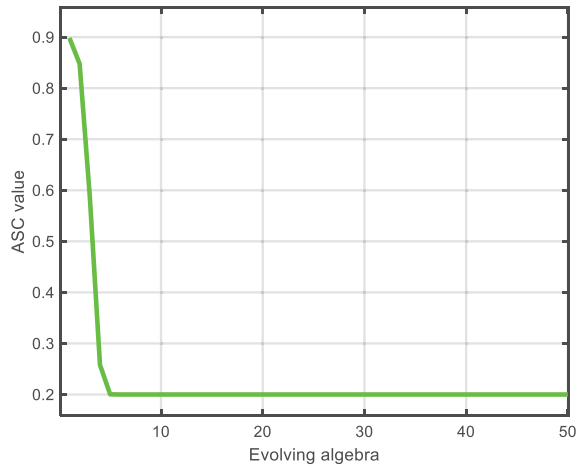

Figure 2. Coefficient *ASC* variation curve

Figure 2 indicates that *ASC* values decrease with the evolving algebra. At the beginning of the evolving algebra, *ASC* value makes crows have stronger global search capacity. At the end of the evolving algebra, *ASC* value is smaller, which makes crows maintain stronger local development ability. *ACS* balances the global and local convergence performance of the proposed algorithm. The updating equation of crow position is as follows.

$$\boldsymbol{Pos}_j^{iter+1} = ASC \times \boldsymbol{Pos}_j^{iter} + R \times FL_j^{iter} \times (m_j^{iter} - \boldsymbol{Pos}_j^{iter}) \tag{13}$$

3.4 Analysis of convergence performance of the ENCSA algorithm

The convergence effects of intelligent algorithms are analyzed by multimodal and unimodal functions (karaboga and Basturk, 2007; mirjalili et al., 2014). The unimodal function has only one global optimal solution. The multimodal function has multiple local solutions. Multimodal function is able to test the global search and local development capabilities of the algorithms. Table 1 presents the expression and solution of the functions.

The moth-flame optimization algorithm (MFO), classical particle swarm optimization algorithm (PSO), CSA and ENCSA algorithm are used to optimize the multimodal and unimodal functions. The PSO, MFO and CSA algorithms belong to the group search algorithm, which completes the search through cooperation between the populations. As a classic algorithm, the PSO algorithm is often used as a comparison algorithm. The PSO algorithm imitates the flight behavior of birds. The MFO algorithm is a novel bionic algorithm with a wide range of applications (Mirjalili, 2015). The MFO algorithm imitates the flight path of moth when it flies to the target. This study uses the MFO algorithm as a comparison algorithm. Table 2 shows the parameter values of PSO, MFO, CSA and ENCSA algorithms.

Table 1. Convergence performance test function of intelligent algorithm

Function attribute	Function expression	Function solution	Variable range
Unimodal	$g_1 = \sum_{j=1}^{\dim} v_j^2$	0	[-100, 100]

	$g_2=\sum_{j=1}^{\dim}(\sum_{k=1}^{j}v_k)^2$	0	[-100, 100]
	$g_3=\sum_{j=1}^{\dim}\lvert v_j\rvert+\prod_{j=1}^{\dim}\lvert v_j\rvert$	0	[-10, 10]
Multimodal	$g_4=\frac{1}{4000}\sum_{j=1}^{\dim}v_j^2-\prod_{j=1}^{\dim}\cos(\frac{v_j}{\sqrt{j}})+1$	0	[-600, 600]
	$g_5=\sum_{j=1}^{\dim}(v_j^2-10\times\cos(2\pi v_j))+10\times\dim$	0	[-5.12, 5.12]
	$g_6=-20\times e^{-0.2\times\sqrt{\frac{1}{n}\sum_{j=1}^{\dim}v_j^2}}+20-e^{\frac{1}{n}\sum_{j=1}^{\dim}\cos(2\pi v_j)}+e$	0	[-32, 32]

Table 2. Parameter setting of three optimization algorithms

Algorithms	Parameters
PSO	*Miter*=1000, N_p=30, C_1=C_2=1.5, *w*=1.4
MFO	*Miter*=1000, *Np*=30, *b*=1
CSA	*Miter*=1000, N_p =30, *FL*=2, *Awp* =0.1
ENCSA	*Miter*=1000, N_p =30, MF=350, *Awp*=0.1, ASC_{max}=0.9, ASC_{min}=0.2

The population size N_P is 30. The maximum number of iterations *Miter* is 1000. In the PSO algorithm, C_1 and C_2 represent learning factors. C_1 represents self-cognition. C_2 represents social experience. In the MFO algorithm, *b* is used to define the spiral shape. In ENCSA, *Awp* represents awareness probability; MF represents migration frequency; ASC represents accelerated search coefficient.

The test dimensions of algorithms are set to 10 and 30. The calculation time and search accuracy of algorithms are analyzed by increasing the test dimension. For each test function, each algorithm runs 30 times. The optimization results and calculation time of the algorithms are recorded. During the test, the same computer platform is used. Table 3 and 4 show the calculation results of each algorithm.

Table 3. Calculation results of unimodal test functions

F	Algorithms	Best 10dim/ 30dim	Average convergence 10dim/ 30dim	Standard Deviation (*std*) 10dim/ 30dim	Average operation time (s) 10dim/ 30dim
g_1	PSO	8.73×10^{-6}/ 748.10	7.98×10^{-1}/ 1.76×10^{3}	0.17/ 665.17	1.22/ 1.29
	MFO	2.69×10^{-33}/ 3.24×10^{-5}	4.16×10^{-30}/ 1.33×10^{3}	1.21×10^{-29}/ 3.45×10^{3}	1.06/ 1.39

	CSA	1.05×10^{-9}/ 2.86×10^{-2}	3.04×10^{-8}/ 8.96×10^{-2}	3.37×10^{-8}/ 4.82×10^{-2}	1.09/ 1.27
	ENCSA	4.67×10^{-72}/ 6.17×10^{-72}	4.78×10^{-67}/ 5.72×10^{-67}	1.09×10^{-66}/ 1.75×10^{-66}	1.26/ 1.25
g_2	PSO	4.28×10^{-2}/ 2.40×10^{3}	8.70/ 5.41×10^{3}	12.37/ 2.11×10^{3}	2.68/ 6.49
	MFO	1.21×10^{-9}/ 377.43	500/ 2.10×10^{4}	2.01×10^{3}/ 1.34×10^{4}	2.61/ 6.47
	CSA	1.35×10^{-5}/ 29.64	5.47×10^{-4}/ 74.43	6.34×10^{-4}/ 25.84	2.64/ 6.36
	ENCSA	9.97×10^{-71}/ 1.88×10^{-71}	6.98×10^{-66}/ 9.13×10^{-63}	3.49×10^{-65}/ 4.99×10^{-62}	2.83/ 6.32
g_3	PSO	3.48×10^{-2}/ 13.49	0.73/ 24.82	0.68/ 9.81	1.23/ 1.32
	MFO	5.54×10^{-21}/ 1.96×10^{-4}	0.66/ 35.61	2.53/ 22.45	1.18/ 1.47
	CSA	5.31×10^{-5}/ 0.42	1.31×10^{-2}/ 1.56	3.70×10^{-2}/ 0.71	1.25/ 1.34
	ENCSA	7.96×10^{-38}/ 6.01×10^{-36}	5.61×10^{-35}/ 2.15×10^{-34}	7.32×10^{-35}/ 3.12×10^{-34}	1.25/ 1.38

Table 3 presented the calculation results of the PSO, MFO, CSA and ENCSA algorithms for unimodal functions. For g_1 to g_3, regardless of the best value, average value and *std*, the ENCSA algorithm obtained better optimization results. When the calculation dimension was 10dim, the calculation results of the PSO, MFO and CSA algorithms were more accurate than when dimension was 30dim. As the number of dimensions increased, the computing power and computing stability of PSO, MFO, and CSA algorithms decreased. For the ENCSA algorithm, the calculation results at 10dim and 30dim were basically consistent, which showed ENCSA had better calculation stability and calculation accuracy. For the average running time of the unimodal function, the difference in running time of the four algorithms was small.

Table 4. Calculation results of multimodal test functions

F	Algorithms	Best convergence 10dim/ 30dim	Average convergence 10dim/ 30dim	Standard Deviation (*std*) 10dim/ 30dim	Average operation time (s) 10dim/ 30dim
g_4	PSO	3.48×10^{-2}/ 6.08	0.73/ 15.19	0.68/ 5.45	1.41/ 1.58
	MFO	3.94×10^{-2}/ 6.19×10^{-5}	0.14/ 12.08	7.67×10^{-2}/ 31.22	1.36/ 1.81
	CSA	1.72×10^{-2}/ 0.12	0.17/ 0.25	9.83×10^{-2}/ 7.93×10^{-2}	1.39/ 1.59
	ENCSA	0/ 0	0/ 0	0/ 0	1.44/ 1.61
g_5	PSO	6.96/ 83.21	15.51/ 118.79	5.54/ 24.67	1.39/ 1.58
	MFO	7.95/ 83.57	19.70/	12.55/ 37.96	1.31/ 1.76

			165.42		
	CSA	2.98/ 10.96	8.45/ 25.38	4.27/ 9.64	1.44/ 1.51
	ENCSA	0/ 0	0/ 0	0/ 0	1.41/ 1.56
g_6	PSO	8.87×10^{-2}/ 7.40	2.99/ 10.61	1.18/ 1.52	1.64/ 1.78
	MFO	4.44×10^{-15}/ 1.50×10^{-3}	0.14/ 14.09	0.45/ 7.72	1.52/ 2.11
	CSA	2.44×10^{-5}/ 2.02	1.43/ 3.50	1.06/ 0.96	1.62/ 1.82
	ENCSA	8.88×10^{-16}/ 8.88×10^{-16}	8.88×10^{-16}/ 8.88×10^{-16}	1.00×10^{-31}/ 1.00×10^{-31}	1.66/ 1.77

The calculation results of the multimodal functions were shown in Table 4. For g_4 to g_6, regardless of the best value, average value and *std*, the calculation results of the ENCSA algorithm were the smallest. For g_4 to g_5, the ENCSA algorithm calculated the optimal solution 0. For multimodal functions, the calculation accuracy of PSO, CSA and MFO algorithms was significantly reduced. The multimodal function has multiple local solutions. The PSO, CSA, and MFO algorithms had poor ability to get rid of the local solutions, which made the algorithm's calculation results worse. For multimodal functions, the ENCSA algorithm exhibited a strong ability to get rid of local solutions. The calculation stability of the ENCSA algorithm was better. For g_4 to g_6, the calculation results of ENCSA algorithm was the same whether it is in 10 or 30 dim.

The average operation time of each algorithm reflects the time complexity of different algorithms. The higher the time complexity of the algorithm, the longer the operation time of the algorithm. For unimodal functions, the average operation time of four algorithms increased with the increase of test dimension. Compared with CSA algorithm, the average operation time of the proposed ENCSA algorithm did not increase significantly. For g_1, the average operation time of the proposed algorithm did not increase when the testing dimension was increased. For g_2, when the testing dimension was increased, the average operation time of CSA algorithm increased by 58.49%, and that of ENCSA algorithm increased by 55.50%. For multimodal testing functions, the average operation time of ENCSA algorithm was close to that of CSA algorithm. For g_4, the average operation time of ENCSA algorithm was higher than that of CSA algorithm. But for g_5 and g_6, when the test dimension was 80, the average operation time of ENCSA algorithm was smaller than that of CSA algorithm. Comprehensive analysis presented that compared with prior algorithms, the complexity of ENCSA algorithm did not increase significantly, and ENCSA algorithm obtained more competitive convergence result.

The calculation result of the ENCSA algorithm was the best according to the calculation values, which indicated that the calculation cost did not increase. The ENCSA algorithm’s regular flight strategy enhances the algorithm's ability to get rid of local solutions. The adaptive flight step size and acceleration search coefficient make the algorithm have strong global search and local development capabilities. Especially for 30dim, the calculation speed of ENCSA algorithm was faster. Compared with the CSA algorithm, the computing power of the ENCSA algorithm had been greatly improved.

This study compares the proposed ENCSA algorithm with state-of-the-art CSA variants, such as PGCSA (Das et al. 2020), ICSA (Lu et al. 2020) and CSA based on opposition learning (Shekhawat and Saxena, 2020). For the benchmark function g_6, when the search dimension was 10, the average convergence value and *std* of the PGCSA algorithm were 2.54×10^{-14} and 2.80×10^{-13}; when the search dimension was 30, the average convergence value and *std* were 7.98×10^{-15} and 2.21×10^{-05}. For the benchmark function g_5, the PGCSA algorithm converged to 0 when the search dimension was 10 or 30. For the benchmark function g_3, when the search dimension was 10, the average convergence value and *std* of the PGCSA algorithm were 2.54×10^{-14} and 2.80×10^{-13}; when the search dimension was 30, the average convergence value and *std* were 7.98×10^{-15} and 2.21×10^{-5}. Lu et al. (2020) set the test dimension to 10 and used the benchmark function g_5 to test the proposed ICSA algorithm.

The optimal convergence value and *std* of ICSA algorithm were 0 and 0.054. Although ICSA algorithm converges to 0, it does not converge to the optimal value every operation. Shekhawat and Saxena (2020) set the test dimension to 30, and used unimodal and multimodal benchmark functions to test the proposed algorithm. For the benchmark function g_1, the average convergence value and std of the proposed algorithm were 1.33×10^{-60} and 2.26×10^{-61}; for g_2, the average convergence value and *std* of the proposed algorithm were 1.36×10^{-06} and 6.87×10^{-06}; for g_3, the average convergence value and *std* of the proposed algorithm were 2.57 and 3.39×10^{-01}; for g_4, the average convergence value and *std* of the proposed algorithm were 5.44×10^{-07} and 2.98×10^{-06}; for g_6, the average convergence value and *std* of the proposed algorithm were 2.91×10^{-08} and 8.91×10^{-08}; and for g_6, the average convergence value and *std* of the proposed algorithm were 4.43×10^{-05} and 1.16×10^{-05}. The benchmark function test results revealed that the convergence performance of the proposed ENCSA algorithm in this study outperformed the state-of-the-art CSA variants.

4. Wind power data acquisition and short-term wind power prediction process

4.1 Data acquisition and analysis of influencing factors

The core business of ENGIE Group includes renewable energy, which is a major participant in French green power production. The installed wind power capacity has reached 1730MW. La Haute Borne wind farm is located in the northeast of France. The wind farm provides opening wind power data sets (Engie, 2018). The wind farm has four wind power generation equipment, namely R80721, R80711, R80790 and R80736. The static information of four wind turbines is listed in Table 5. ENGIE provides two opening data sets. One data set counts the power generation information of four wind turbines from 2013 to 2016, and the other data set counts the power generation status of each wind turbine from 2017 to 2020. Among them, statistical information includes generator technical parameters and meteorological information. Generator technical parameters include rotor speed, cabin temperature, torque, and pitch angle, etc. Meteorological information includes wind speed, temperature, direction, etc. This study uses the data set recorded by R80711 power generation equipment. The power generation equipment records data every 10 minutes. The daily wind power statistics include 144 data points. The statistical parameters include power, blade position, outdoor temperature, grid voltage, wind speed, grid frequency and other parameters.

This study selects the wind power data in spring, winter and autumn of 2017 as the simulation experiment samples. The statistical ranges intervals of wind power in spring,

autumn and winter are from November 21 to November 26, from April 15 to April 20, and from December 8 to December 13. The selected sample data include 6-day statistics with a total of 864 sets of data. The wind power data of the first five days are taken as the training samples of the forecasting models. The wind power data of the sixth day are taken as the test samples of the model.

The statistical data include voltage, frequency, blade position and other parameters. Wind direction and wind speed directly affect the output power. Wind is a phenomenon of air flow, because the sun's irradiance on the earth's surface is not uniform. The change of temperature affects the change of air density, thus affecting the air flow through the fan blades and resulting in the change of output power of wind power equipment. Therefore, the output variable is the wind power. The input variables are outdoor temperature, wind direction and wind speed.

Table 5. Static information of La Haute Borne wind turbine

Information	La Haute Borne wind turbine			
	R80711	R80721	R80736	R80790
Name	FRHBO_E01_80711	FRHBO_E03_80721	FRHBO_E04_80736	FRHBO_E02_80790
Model	MM82	MM82	MM82	MM82
Manufacture	Senvion	Senvion	Senvion	Senvion
Rotor diameter (m)	82	82	82	82
Hub height (m)	80	80	80	80
Rated power (kW)	2050	2050	2050	2050
Altitude	411	411	411	411
GPS	48.4569,5.5847	48.4497,5.5869	48.4461,5.5925	48.4536,5.5875
Commissioning date	2009/01/15	2009/01/15	2009/01/15	2009/01/15
Department	Meuse	Meuse	Meuse	Meuse
Region	Grand Est	Grand Est	Grand Est	Grand Est

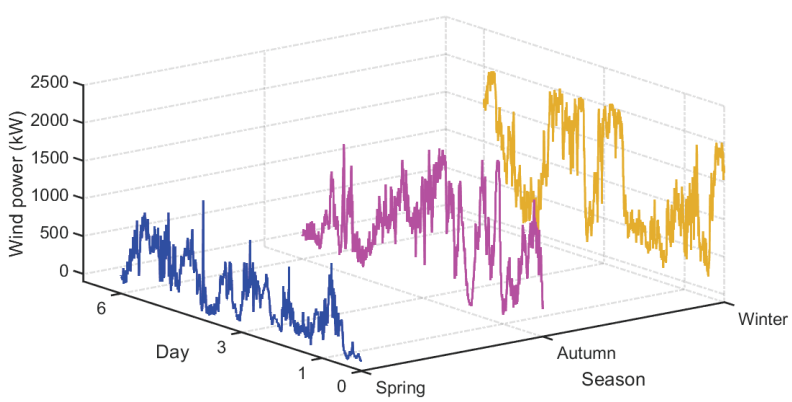

Figure 3. Power curve

The wind power curves shown in Figure 3 are highly nonlinear. The wind speed has strong uncertainty and nonlinearity and shows a large difference in a short time. The wind power shows strong nonlinearity. The wind speed fluctuates with seasons, and wind power is different in different seasons.

4.2 Wind power forecast process

Section 3.1 presents the principle of the ELM model. Thresholds and weights are initialized randomly in the ELM model. This method cannot guarantee the validity of the threshold and weight values, resulting in poor prediction stability of the ELM model. At the same time, the random thresholds and weights affect the training accuracy. In view of the shortcomings of the ELM model, the random parameter values are determined by the ENCSA algorithm. The forecast stability and accuracy are improved.

Variance is used as the training objective function.

$$Func_{objective} = \frac{\sum_{i=1}^{m}(pre_i - act_i)^2}{m} \tag{14}$$

where *pre* is the forecasting value of wind power during training; *act* is the actual wind power value during training.

The operation steps of wind power forecast are shown below:

(1) Determine the output and input variables of the wind power prediction model.
(2) Divide the wind power training samples and wind power test samples of the prediction models.
(3) Perform normalized preprocessing on sample data such as wind power.
(4) Set the relevant parameter values of the wind power forecast models.
(5) Use wind power training samples to train the model.
(6) Calculate the model objective function.
(7) Input the optimized random parameter values into the ELM model.
(8) Predict short-term wind power and denormalize the prediction results.
(9) Analyze and evaluate the forecast results.

Figure 4 shows the flow chart of wind power forecasting.

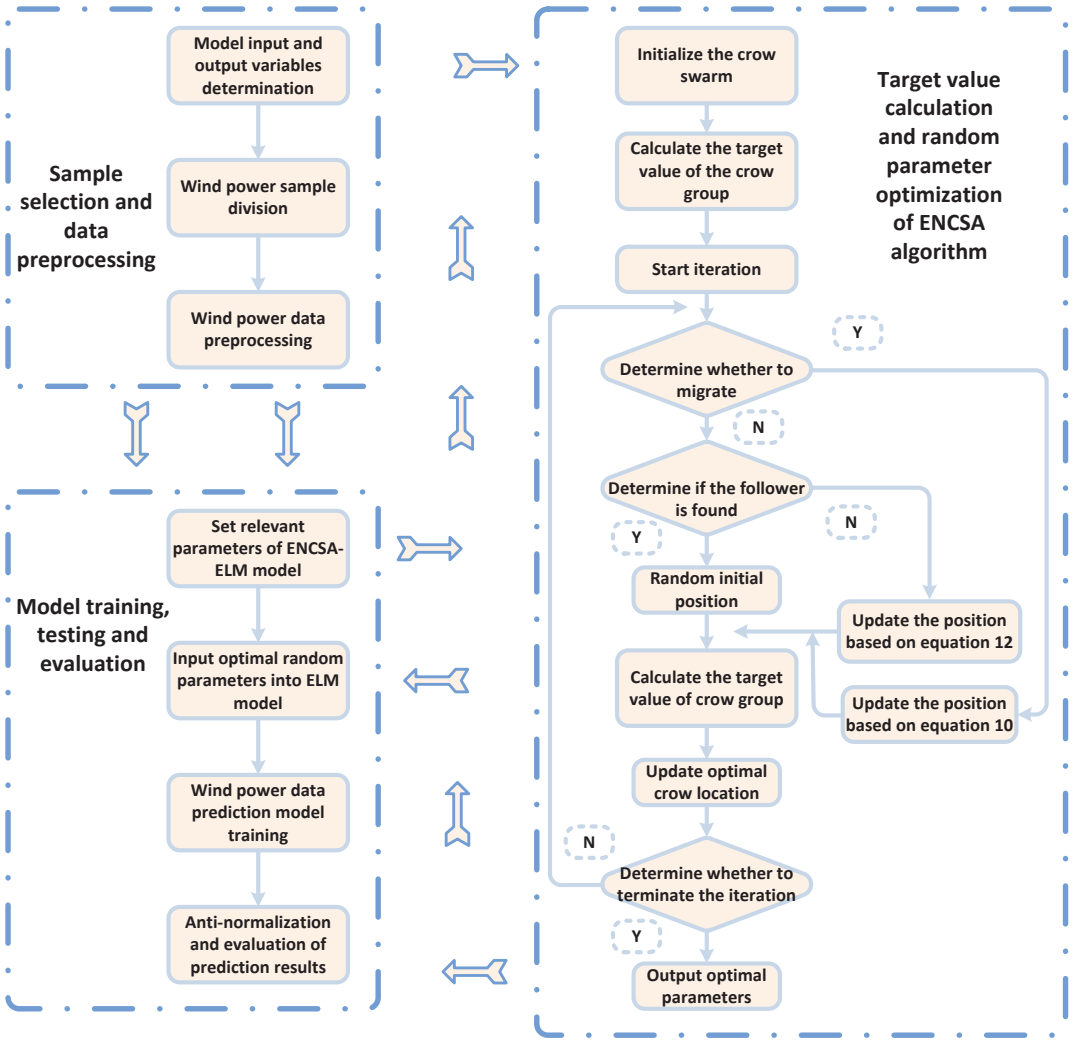

Figure 4. Wind power prediction process

5. Simulation test and results evaluation

5.1 Evaluation index of wind power forecast results

In this study, the forecast results were evaluated by multiple indicators. *RMSE* reflects the deviation between the forecast values and the actual values and also reflects the degree of dispersion between samples. *RMSE* and *MAPE* reflect the forecast error. The smaller the *MAPE* and *RMSE* values are, the higher the forecast accuracy of the model is. R^2 reflects the fitting degree of prediction curve and real value curve. When the value of R^2 is close to 1, it indicates that the model has a good fitting effect. When the value of R^2 is close to 0, it indicates that the model has a poor fitting effect.

$$RMSE = \sqrt{\frac{1}{num}\sum_{i=1}^{num}(pre_i - act_i)} \tag{15}$$

$$MAPE = \frac{100\%}{num} \times \sum_{i=1}^{num}\left|\frac{pre_i - act_i}{act_i}\right| \tag{16}$$

$$R^2 = 1 - \frac{\sum_{i=1}^{num}(pre_i - act_i)^2}{\sum_{i=1}^{num}(act_i - \overline{pre})^2} \tag{17}$$

where $\overline{pre}$ represents the average of the predicted value; pre_i represents the predicted value; act_i represents the actual value.

5.2 Simulation and discussion

The simulation experiments were carried out to verify the predict performance of the ENCSA-ELM model in this section. This study selected three common models as comparative models to forecast wind power. The three comparison models were SVM, Gaussian process regression (GPR), BPNN, ELM, ELM optimized by MFO (MFO-ELM) and ELM optimized by gray wolf optimization algorithm (GWO-ELM) models.

For the sample division, there is no definite method to divide training samples and test samples. The number of data in the training sample set usually accounts for 66.67% to 80% of the total, that is to say, the ratio of the number of data in the training set to the number of data in the test set is 1:2 to 1:4. Zhou et al. (2021) set the ratio of training data to test data to 4:1 in the process of predicting short-term wind power. Li et al. (2020) set the ratio of wind power training samples to test samples to 3:1. Duan et al. (2021) set the ratio of training samples to test samples to 9:1 when verifying the proposed model. With reference to the sample division method given in the above research, this paper sets the ratio of training samples to test samples to 5:1. Therefore, in this study, the training set contains 720 sample points, and the test set contains 144 sample points.

The short-term wind power in spring was forecasted by the ENCSA-ELM, CSA-ELM, BPNN, GPR, SVM, ELM, MFO-ELM and GWO-ELM models. The 720 groups of wind power data from April 15, 2017 to April 19, 2017 were taken as training samples of forecast models. The 144 groups of wind power data collected on April 20, 2017 were used as test data of forecast models. The input variables of the forecast models were wind direction, external temperature and wind speed. The wind power was selected as output variable. Figure 5 depicts the wind power predictive results and errors on April 24, 2017.

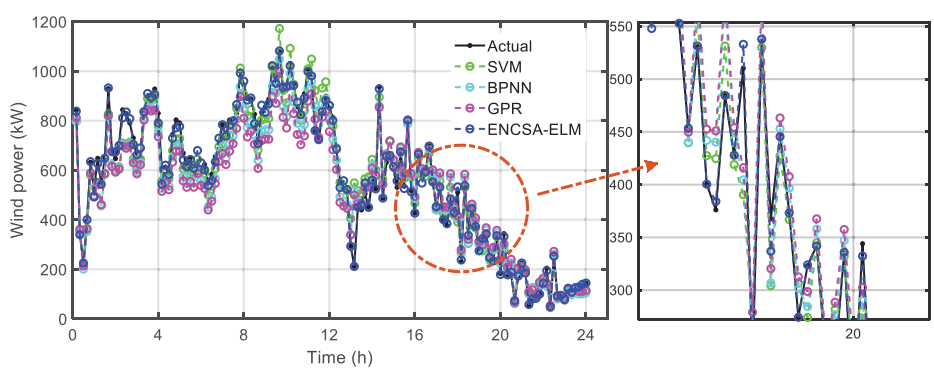

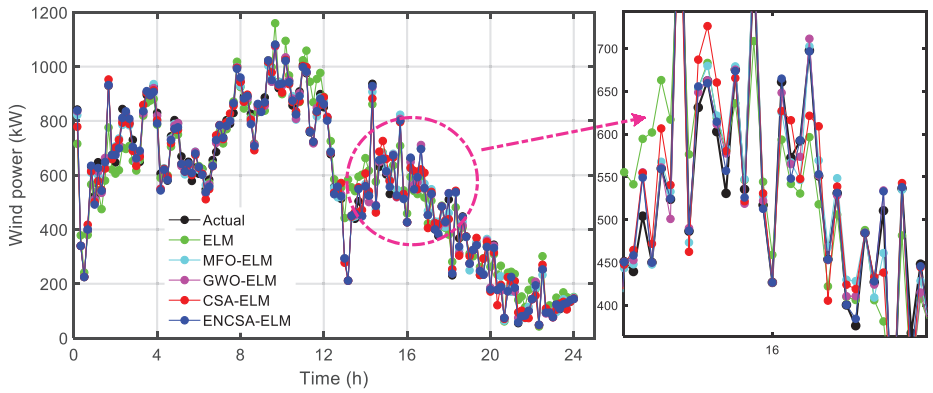

(a) Power prediction curves

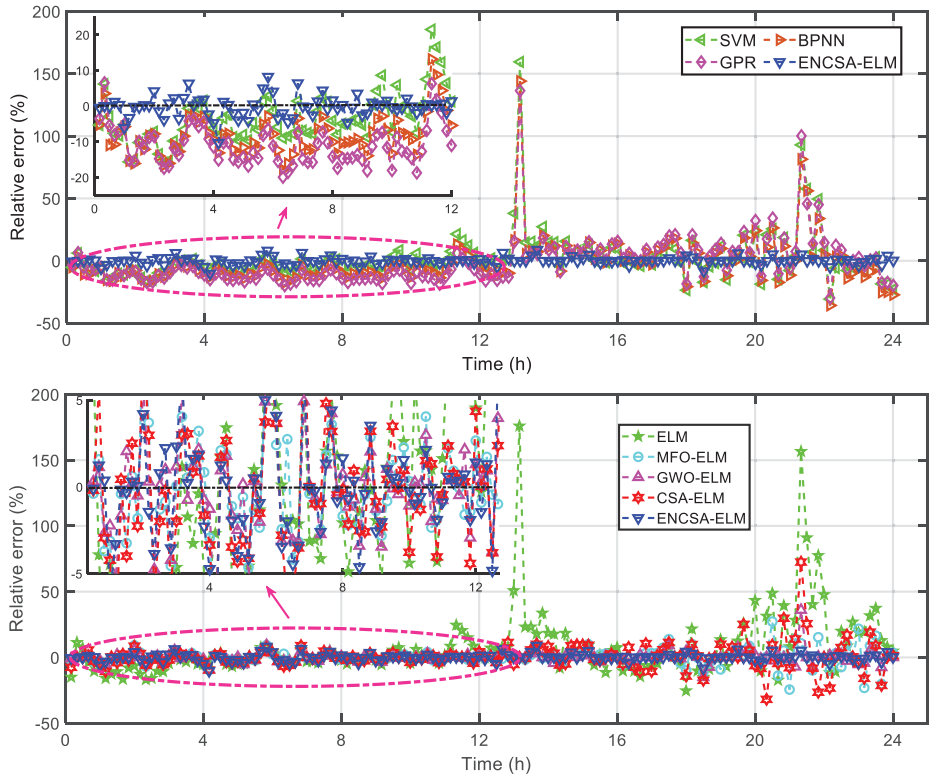

(b) Wind power prediction error

Figure 5. Wind power forecast results on April 20

Figure 5 (a) showed the wind power forecasting curves of SVM, BPNN, GPR, CSA-ELM, ELM, MFO-ELM, GWO-ELM and ENCSA-ELM models for April 20th. The eight forecasting models all presented strong forecasting stability and reflected the fluctuation state of wind power. Figure 5 (b) presented the forecasting errors of eight models. The forecasting errors of the ENCSA-ELM model were the smallest. The ENCSA-ELM model exhibited a high prediction accuracy. The predicted wind power values of the ENCSA-ELM model were closest to the actual values of wind power, and the *RE* values were controlled within |20%|. From 20:00 to 24:00, the prediction errors of SVM, GPR, BPNN and CSA-ELM models become larger, and the *RE* values exceeded 20%.

As shown in Figure 5(b), the prediction errors of SVM, GPR, BPNN, and ELM models had spikes. There are two reasons for spikes: (1) the wind power sequence itself has strong

randomness and volatility, which brings challenges to the predictive stability and accuracy of the forecasting models; and (2) the random parameters in the machine learning models have a greater impact on the prediction stability of the model. However, SVM, GPR, BPNN, and ELM models themselves have no method to solve random parameters. Based on the above two reasons, traditional machine models may have large errors in the process of predicting wind power. In order to reduce the spikes in the prediction results, it is necessary to select the optimal parameters of the machine learning model. The predictive performance of CSA-ELM, MFO-ELM, GWO-ELM and ENCSA-ELM models outperformed ELM model, indicating that parameter optimization improved the forecasting accuracy and stability of ELM model. The proposed model exhibited a higher predictive stability. The prediction error distribution of each model is depicted in Figure 6 and Table 6.

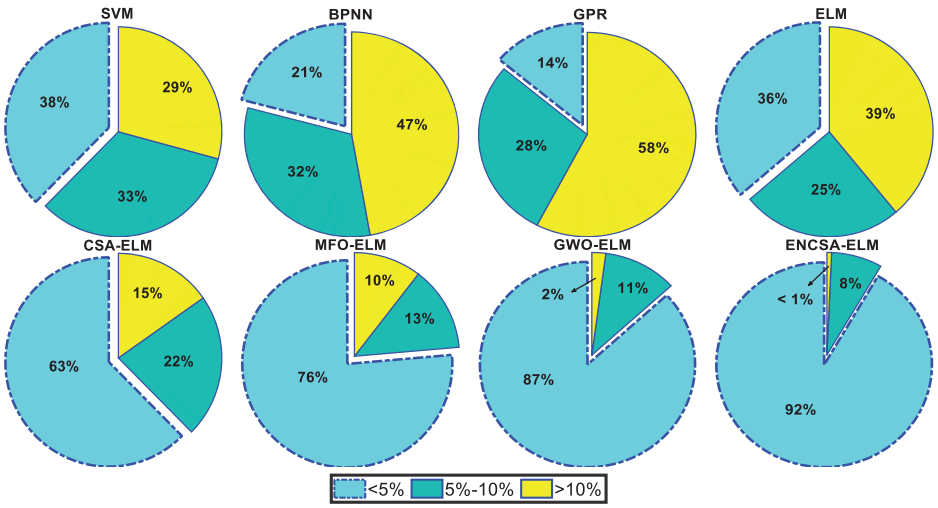

Figure 6. Prediction error statistics on April 20

Table 6. Error distribution of wind power of five models on April 20

Model	Number				
	$\|RE\|<5\%$	$5\%\le\|RE\|<10\%$	$10\%\le\|RE\|<15\%$	$15\%\le\|RE\|\le20\%$	$\|RE\|>20\%$
SVM	54	48	13	15	14
BPNN	30	46	43	13	12
GPR	20	41	42	31	10
ELM	52	36	19	13	24
CSA-ELM	90	32	10	4	8
MFO-ELM	110	19	8	2	5
GWO-ELM	125	16	1	1	1
ENCSA-ELM	132	11	1	0	0

Figure 6 showed the percentage of relative error absolute values ($|RE|$) in each interval. Table 6 presented the number of predicted values in the error interval. ENCSA-ELM model obtained more satisfactory forecasting results by analyzing error distribution in Table 6. Figure 6 indicated the number of error values of proposed model in the interval $|RE|<5\%$ exceeded 90%. The prediction errors of proposed model were all controlled within 15%. The number of

error values of elm model in the interval |*RE*|<5% accounted for 36% of the total. The error values of MFO-ELM, CSA-ELM and GWO-ELM models in the interval |*RE*|<5% accounted for 76%, 63% and 87% of the total respectively. The *RE* values of BPNN and GPR models in the interval [- 5%, 5%] accounted for the smallest proportion of the total, which were 21% and 14% respectively.

The wind power in autumn was forecasted by the SVM, BPNN, GPR, ELM, MFO-ELM, GWO-ELM, CSA-ELM and ENCSA-ELM models. The 720 sets of wind power data collected from November 21, 2017 to November 25, 2017 were selected as the training samples for eight prediction models, and the 144 sets of wind power data collected on November 26, 2017 were taken as the test data. Figure 7 presents the forecast results of each model for the 24-hour wind power on the 26th of autumn.

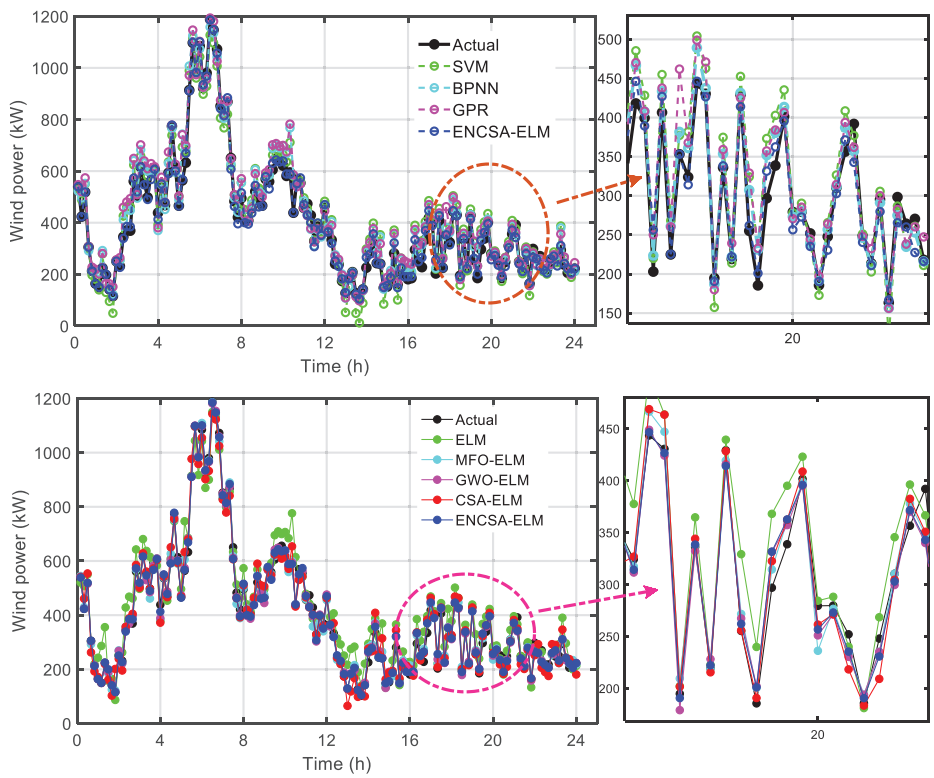

(a) Power prediction curves in autumn

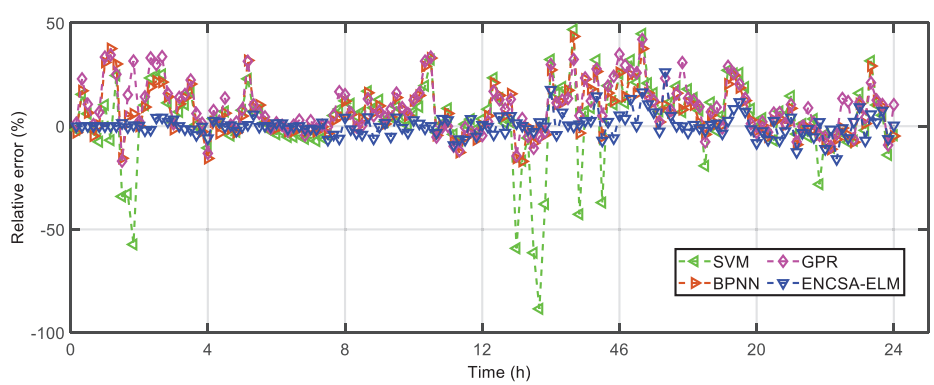

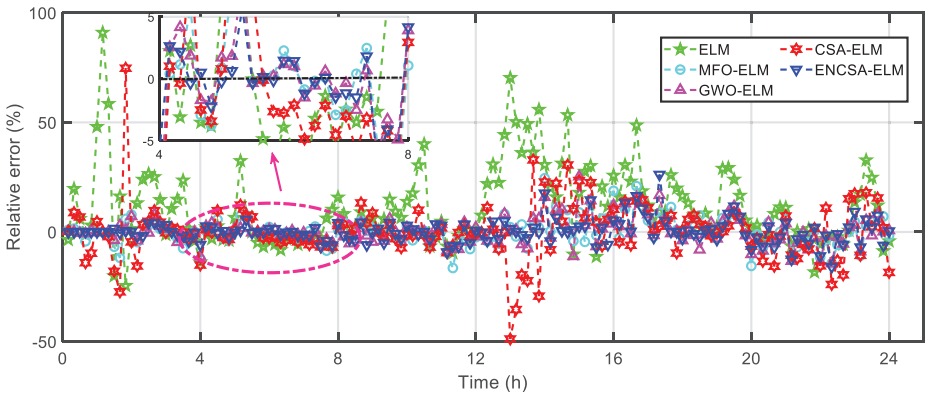

(b) Wind power prediction error in autumn

Figure 7. Wind power forecast results on November 26

Figure 7 (a) revealed the forecasting results for autumn wind power. The forecasting curves were consistent with the trend of the actual wind power curve. On the whole, the predicted values of the eight models fitted well with the true values. Figure 7 (b) presented the hourly forecast error of each forecast model for autumn wind power. The ENCSA-ELM model still exhibited a high prediction accuracy. Only a few of *RE* values exceeded 20%. Most of the error values were controlled within 20%. A large number of error values of SVM, BPNN, GPR, ELM, MFO-ELM and CSA-ELM prediction models exceeded 20%. For BPNN model, the maximum *RE* exceeded 80%. The maximum *RE* of the CSA-ELM model exceeded 60%. The prediction stability of the ELM model was poor, and the *RE* at multiple moments exceeded 50%. For autumn wind power, the predictive stability and prediction accuracy of the proposed model were better. Figure 8 and Table 7 reveal the relative error distribution of each model.

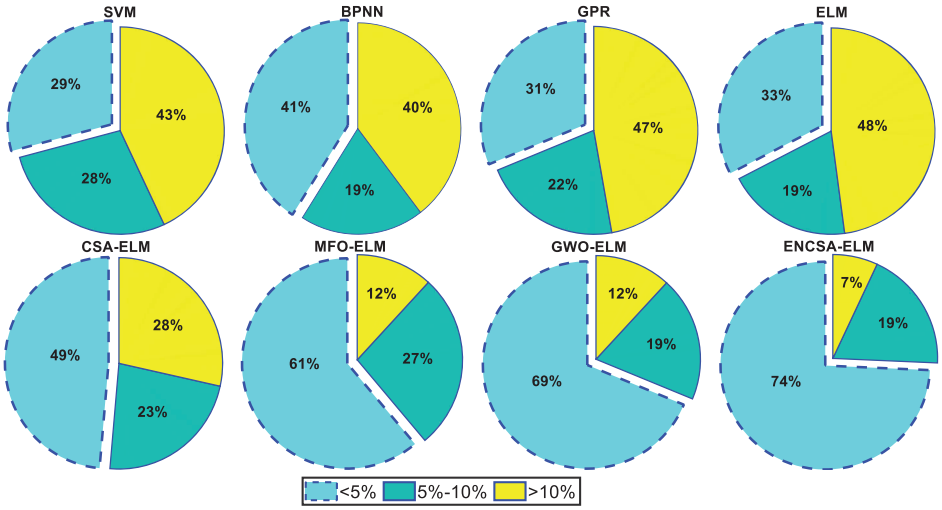

Figure 8. Forecast error statistics on November 26

Table 7. Error distribution of wind power of eight models on November 26

Model	Number				
	$\|RE\|<5\%$	$5\%\le\|RE\|<10\%$	$10\%\le\|RE\|<15\%$	$15\%\le\|RE\|\le20\%$	$\|RE\|>20\%$
SVM	42	40	18	15	29

BPNN	59	28	22	15	20
GPR	45	31	29	11	28
ELM	47	28	17	13	39
CSA-ELM	70	33	16	12	13
MFO-ELM	88	39	12	3	2
GWO-ELM	99	28	13	3	1
ENCSA-ELM	107	27	6	3	1

Figure 8 depicted the prediction errors of eight models for wind power in autumn. The number of error values in the interval [-5%, 5%] of the proposed model accounted for the highest proportion of total samples, exceeding 70%. CSA-ELM, MFO-ELM and GWO-ELM models obtained more satisfactory predictive results compared with ELM model. The error values in the interval $|RE|<5\%$ of CSA-ELM, MFO-ELM and GWO-ELM models accounted for 49%, 61% and 69% of the total samples, but only 33% of the *RE* of the ELM model was in the interval [-5%, 5%]. The error values of SVM, BPNN and GPR models in the interval $|RE|<5\%$ accounted for 29%, 41% and 31% of the total samples. The prediction error of ENCSA-ELM model was relatively small. Table 7 listed the *RE* error distribution of the eight forecast models. The prediction errors of proposed model were basically controlled within 10% compared with other models. For 144 sample points, the $|RE|$ errors of 107 sample points of proposed model were smaller than $|5\%|$, and only one sample point error exceeded 20%.

The wind power in winter was predicted by the SVM, BPNN, GPR, ELM, MFO-ELM, GWO-ELM, CSA-ELM and ENCSA-ELM models. The 720 sets of wind power data collected from December 8, 2017 to December 12, 2017 were taken as the training samples for eight prediction models. The 144 sets of wind power data collected on December 13, 2017 were selected as the test data. Figure 9 depicts the forecasting effects.

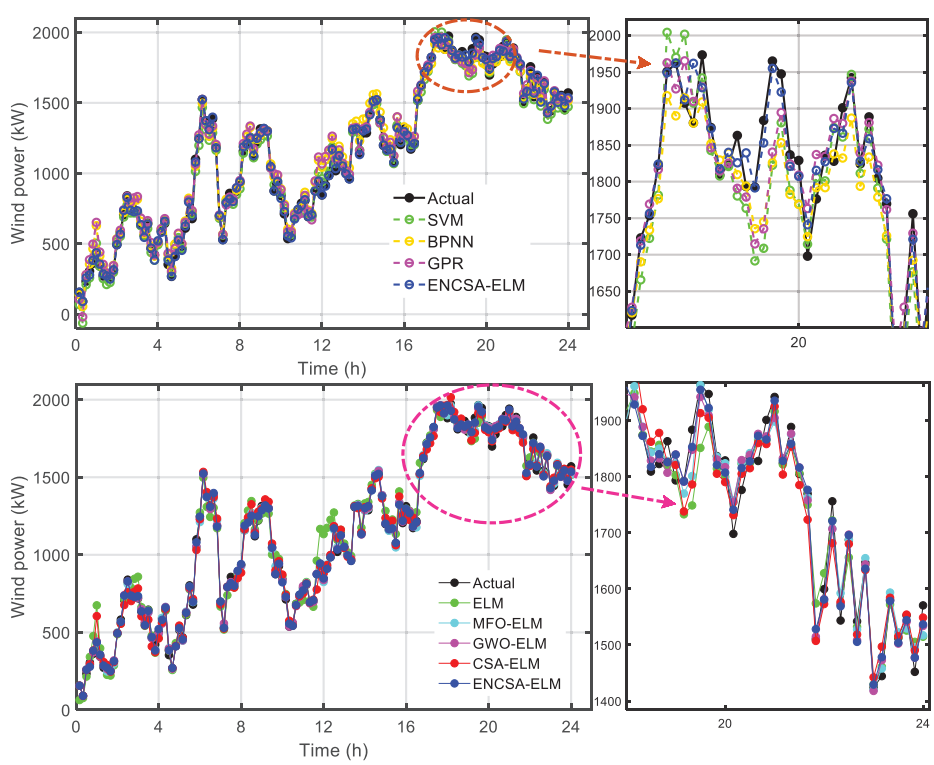

(a) Power prediction curves in winter

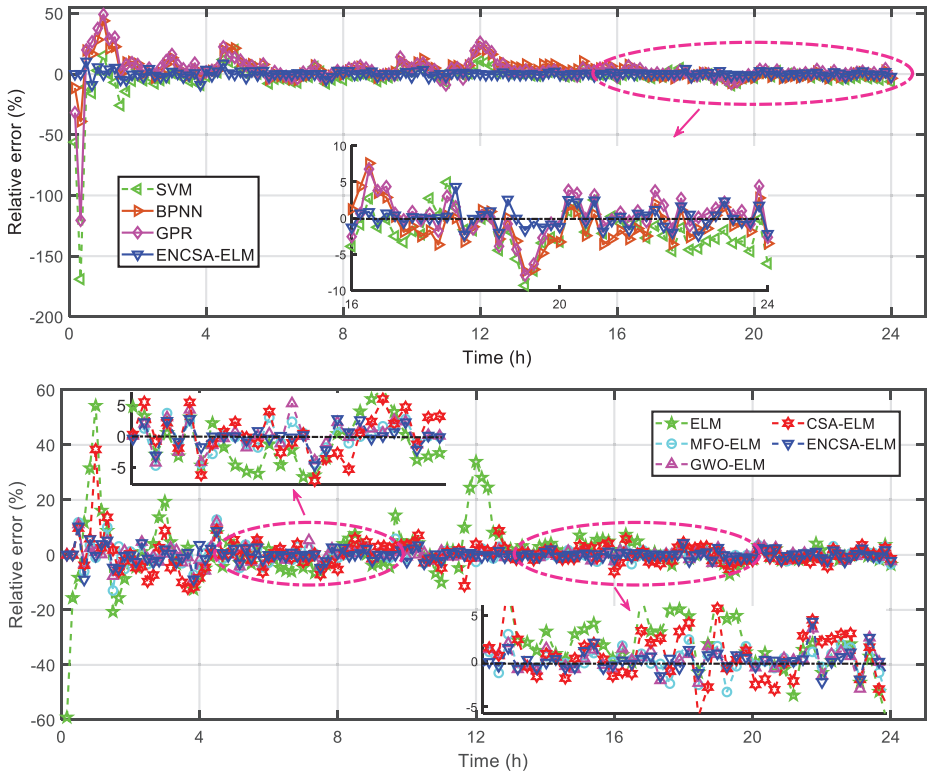

(b) Wind power prediction error in winter

Figure 9. Wind power forecast results on December 13

Figure 9 presented the forecasting curves for winter wind power. The local enlarged drawing in Fig. 9 showed that the predicted curve of ENCSA-ELM model was closest to the actual power curve. In the initial stage of prediction, SVM and GPR model had a large deviation from the actual value. For SVM model, the maximum relative error exceeded 150%. The maximum relative error of the GPR model exceeded 100%. Compared with CSA-ELM, MFO-ELM, GWO-ELM and ENCSA-ELM models, the prediction curve of the ELM model fluctuated more, and the maximum *RE* exceeded 50%. Figure 9 (b) revealed that the ENCSA-ELM model showed high predictive stability and *RE* errors fluctuated smoothly. Figure 10 and Table 8 depicted the relative error distribution of each forecasting model.

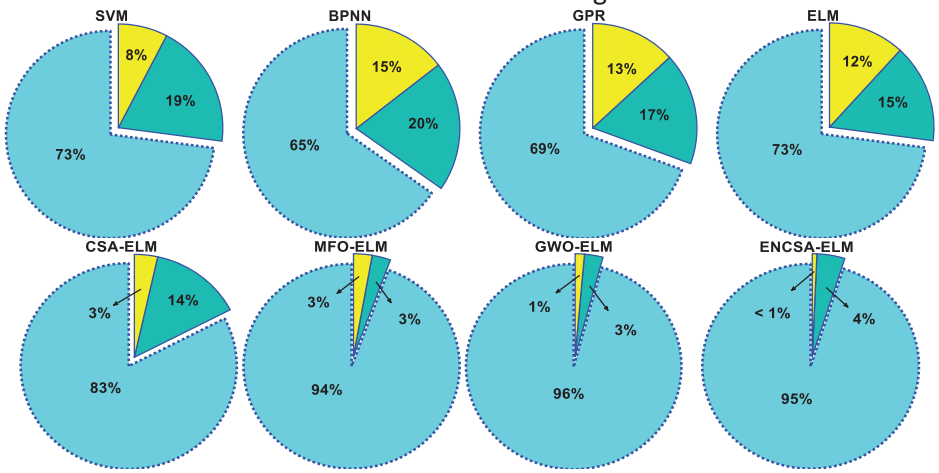

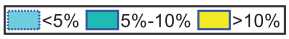

Figure 10. Forecast error statistics on December 13

Table 8. Error distribution of wind power of eight models on December 13

Model	Number				
	$\|RE\|$<5%	5%≤$\|RE\|$<10%	10%≤$\|RE\|$<15%	15%≤$\|RE\|$≤20%	$\|RE\|$>20%
SVM	105	28	5	3	3
BPNN	94	29	7	6	8
GPR	100	25	5	4	10
ELM	105	22	5	4	8
CSA-ELM	119	20	4	0	1
MFO-ELM	136	4	4	0	0
GWO-ELM	138	4	2	0	0
ENCSA-ELM	137	6	1	0	0

Figure 10 revealed that compared with other prediction models, GWO-ELM and ENCSA-ELM models got satisfactory prediction results. The error values of the GWO-ELM and proposed models in the interval $|RE|$<5% accounted for 96% and 95% of the total samples. The error values of SVM, BPNN, GPR, ELM, MFO-ELM and CSA-ELM models in the interval $|RE|$<5% accounted for 73%, 65%, 69%, 73%, 94% and 83% of the total samples. The prediction errors of the ENCSA-ELM model basically were within the [-5%, 5%] interval. Table 8 listed the prediction error distribution of the eight models. For 144 sample points, the error of 137 sample points of proposed model was less than 5%, and no error was more than 20%. The predictive errors of proposed model were controlled within 10%.

As the complexity of the algorithm is higher, the time frequency is greater, and the running time required by the algorithm is longer. Therefore, this paper takes the running time of the algorithm as an evaluation index to analyze the complexity of each algorithm. Table 9 and Figure 11 revealed the evaluation results of different wind power prediction models.

Table 9. Evaluation of model prediction results

Season	Model	Evaluation index			
		RMSE	*MAPE* (%)	R^2 (%)	Running time (s)
Spring	SVM	59.17	10.37	95.31	0.25
	BPNN	66.52	11.71	95.33	0.28
	GPR	79.71	13.22	94.40	11.45
	ELM	67.26	13.69	94.03	1.59×10^{-3}
	CSA-ELM	29.93	5.96	98.79	19.14
	MFO-ELM	22.15	4.15	99.34	19.33
	GWO-ELM	17.31	2.46	99.60	20.48
	ENCSA-ELM	**16.45**	**1.88**	**99.64**	19.59
Autumn	SVM	49.42	13.12	96.11	0.26
	BPNN	46.28	9.78	97.02	0.30
	GPR	52.08	11.56	96.88	12.75
	ELM	58.20	14.80	95.50	2.82×10^{-3}

	CSA-ELM	32.15	8.44	98.10	18.02
	MFO-ELM	20.55	4.64	99.22	18.53
	GWO-ELM	18.71	4.35	99.35	19.19
	ENCSA-ELM	**17.13**	**3.59**	**99.46**	18.47
Winter	SVM	48.01	5.27	99.23	0.26
	BPNN	60.37	5.76	98.96	0.39
	GPR	60.16	6.40	98.92	11.70
	ELM	65.94	5.53	98.42	1.61×10^{-3}
	CSA-ELM	38.92	3.22	99.43	18.58
	MFO-ELM	22.32	1.87	99.81	18.31
	GWO-ELM	20.42	1.62	99.84	19.34
	ENCSA-ELM	**18.60**	**1.49**	**99.87**	18.60

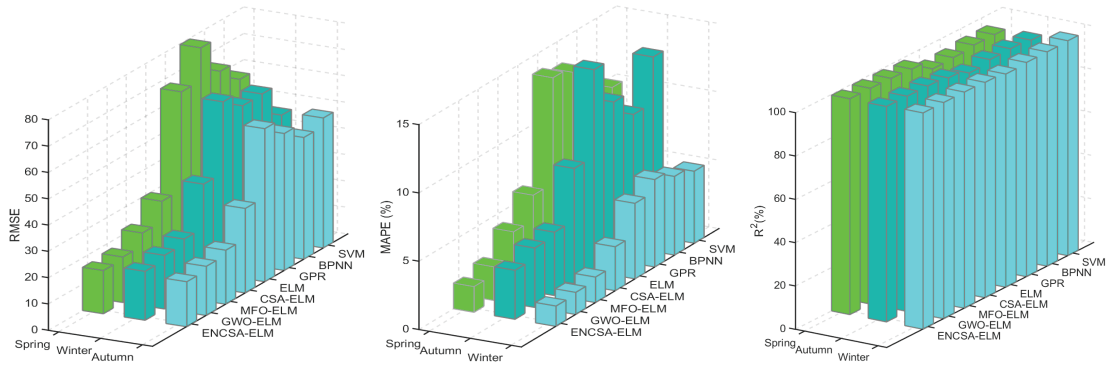

Figure 11. Model prediction error comparison

Table 9 listed the evaluation results of the eight wind power prediction models. The comparison results of the evaluation indexes of wind power forecasting were depicted in Figure 11. The *RMSE* value of the ENCSA-ELM model was controlled below 20 in different seasons. Compared with traditional machine learning models, the *RMSE* and *MAPE* values were the smallest. For spring wind power forecasting, the *MAPE* value was 8.49%, 9.83% and 11.34% smaller than that of the SVM, BPNN and GPR models. For the prediction results of the wind power in autumn, the *MAPE* value of ENCSA-ELM model was 9.53%, 6.19% and 7.97% smaller than that of the SVM, BPNN and GPR a models. For the forecasting results of winter power, the *MAPE* value of ENCSA-ELM model was 3.78%, 4.27% and 4.91% smaller than that of the SVM, BPNN and GPR models. Similarly, compared with ELM, CSA-ELM, MFO-ELM and GWO-ELM models, the proposed model obtained more satisfactory wind power forecasting results.

The ELM model prediction performance was obviously improved when random parameters were optimized by the optimization algorithms. For wind power prediction results in different seasons, the average *RMSE* of ENCSA-ELM model was 17.39, which was 1.42, 4.28 and 16.28 smaller than those of GWO-ELM, MFO-ELM and CSA-ELM models. The average *MAPE* of ENCSA-ELM model was 2.32%, which was 0.49%, 1.23% and 3.55% smaller than those of GWO-ELM, MFO-ELM and CSA-ELM models. For R^2, the R^2 values of the eight models reached more than 90%. The ENCSA-ELM model had the highest R^2. Both of the two evaluations of the proposed model's R^2 reached more than 99%. The evaluation results

revealed that the ENCSA-ELM model had the highest forecasting accuracy. The proposed model still achieved better evaluation results compared with other models.

ELM model consumed the shortest running time compared with the traditional machine learning models. The training time of the model is greatly shortened because ELM does not use gradient descent method. The running time of the model became longer when the ELM model was combined with optimization algorithms. This is because the algorithms need to optimize the random parameters of the ELM model in the training process, which increases the training time of the model. CSA-ELM, GWO-ELM, MFO-ELM and ENCSA-ELM models consumed similar running time, indicating that the four models had similar time complexity. The GWO-ELM model consumed slightly more time than the other three models. The running time of the ENCSA-ELM model was slightly higher than that of the CSA-ELM model, indicating that the complexity of the proposed ENCSA-ELM model did not increased significantly. The evaluation results in Table 9 revealed that compared with the traditional machine learning models and the ELM optimized by different algorithms, the proposed model obtained more competitive prediction accuracy and fitting effect. Regarding the time complexity, the running time consumed by the proposed model was slightly higher than that of the CSA-ELM model, but less than that of the GWO-ELM model. Comprehensive analysis demonstrated that the wind power forecast results obtained by the proposed model were the most competitive compared with the other seven models.

This study compares the proposed model with the state-of-the-art short-term wind power prediction models in order to further verify the effectiveness of the proposed ENCSA-ELM model. For example, Duan et al. (2021) proposed a hybrid short-term wind power prediction model and resulted the evaluation index RMSE 58.77. Liu et al. (2020) developed WD-LSTM model to forecast wind power, the MAPE of the proposed model was 5.83. Tu et al. (2020) proposed the DR-SVM model to predict wind power in different seasons. For wind power in winter, spring and autumn, the MAPE values of the DR-SVM model were 6.86%, 15.31%, and 9.39%, respectively. Li et al. (2020) proposed the WD-IASO-SVM model to predict short-term wind power, and used two sets of simulation experiments to verify the proposed model. For Cases 1 and 2, the MAPE values of the proposed models were 5.43% and 9.26% respectively. Huang et al. (2020) formulated the OWDPC-LSTM model to forecast short-term wind power. The MAPE values of the proposed OWDPC-LSTM model were 4.09% and 5.85 when the number of cluster centers were 3 and 4. Compared with the state-of-the-art short-term wind power prediction models proposed above, the wind power prediction result obtained by the ENCSA-ELM model are more competitive. Therefore, the model proposed in this study provides a new method for short-term wind power forecasting.

6. Concluding remarks

To meet the balance of power supply and demand, the power sector needs to formulate a reasonable dispatch plan to ensure the economy and safety of the power supply of the power system. The wind power anti-peak-shaving characteristic brings the challenges to grid-dispatching plan when wind power is connected to the grid on a large scale. When the prediction accuracy of wind power is not enough, the grid can stabilize the impact of wind power output fluctuation on power supply stability by setting aside enough spinning reserve capacity. The additional spinning reserve capacity not only increases the operating cost of the grid, but also brings hidden dangers to the grid stable operation. The power sector can formulate dispatch plans more reasonably through high-precision wind power forecasting and

reference to the load forecast values obtained, thereby effectively reducing the spinning reserve capacity reserved for stabilizing wind power volatility and reducing the operating cost of the power system. This study proposes the ENCSA-ELM model to predict the short-term wind power. Meanwhile, traditional machine learning models such as SVM, ELM, BPNN, GPR and ELM models optimized by different intelligent algorithms are selected as the comparison methods. The concluding remarks are presented as follows.

- The ENCSA algorithm was proposed to improve the CSA algorithm limitations. After testing, the convergence accuracy of the ENCSA algorithm was improved obviously. For multimodal functions, the ENCSA algorithm exhibited good convergence accuracy. The abilities of local development and global search of the ENCSA algorithm were strengthened.
- The ENCSA-ELM model was proposed. The *RE* values were controlled within |20%|, the R^2 values were over 99% and the *MAPE* value was controlled under 10%.
- The forecast results of proposed model were analyzed by evaluation indexes. The results revealed that compared with the SVM, GPR, BPNN and CSA-ELM models, the ENCSA-ELM model exhibited higher prediction stability and accuracy.
- Improving the prediction accuracy of wind power can reduce the phenomenon of wind abandonment and assist the power department to formulate a reasonable dispatch plan.

The proposed prediction model achieved high prediction accuracy for short-term wind power. The proposed wind power forecast system had some limitations. The proposed ENCSA algorithm cannot all converge to the global optimal value for unimodal and multimodal test functions, and the convergence performance of the proposed algorithm needs to be further improved. This study only analyzes the influence of temperature, wind direction and wind speed on wind power. Less external factors are considered. Finally, the potential of ENCSA-ELM model is tapped to improve the generalization ability of the proposed model. The limitations of the proposed wind power forecast system will be solved in future research.

Acknowledgements

This study was supported by the key project of Tianjin Natural Science Foundation [Project No. 19JCZDJC32100], the Hebei Provincial Innovation Foundation for Postgraduate [Project No. CXZZBS2020028] and the Natural Science Foundation of Hebei Province of China [Project No. E2018202282].

References

Askarzadeh, 2016 Askarzadeh A.
A novel metaheuristic method for solving constrained engineering optimization problems: Crow search algorithm
Computers & Structures, 169 (2016), pp. 1-12.

Barbounis et al., 2006 Barbounis T.G., Theocharis J.B., Alexiadis M.C., Dokopoulos P.S. 2006.
Long-term wind speed and power forecasting using local recurrent neural network models
IEEE Transactions on Energy Conversion, 21(2006), pp. 273-284.

Chen and Liu, 2020 Chen C., Liu H.
Medium-term wind power forecasting based on multi-resolution multi-learner ensemble and adaptive model selection

Energy Conversion and Management, 206 (2020), 16.
Cassola and Burlando, 2012 Cassola F. Burlando M.
Wind speed and wind energy forecast through Kalman filtering of Numerical Weather Prediction model output
Applied Energy, 99 (2012), pp. 154-166.
Cai et al., 2020 Cai H.S., Jia X.D., Feng J.S., Li W.Z., Hsu Y.M., Lee J.
Gaussian Process Regression for numerical wind speed prediction enhancement
Renewable Energy, 146 (2020), pp. 2112-2123.
Catalao et al., 2011 Catalao J.P.S., Pousinho H.M.I., Mendes V.M.F.
Hybrid intelligent approach for short-term wind power forecasting in Portugal
IET Renewable Power Generation, 5(2011), pp. 251-257.
Chen et al., 2014 Chen N.Y., Qian Z., Nabney I.T., Meng X.F.
Wind Power Forecasts Using Gaussian Processes and Numerical Weather Prediction
IEEE Transactions on Power Systems, 29(2014), pp. 656-665.
Choudhary and Shukla, 2021 Choudhary R., Shukla S.
A clustering based ensemble of weighted kernelized extreme learning machine for class imbalance learning
Expert Systems with Applications, 164 (2021).
Dupre et al., 2020 Dupre A., Drobinski P., Alonzo B., Badosa J., Briard C., Plougonven R.
Sub-hourly forecasting of wind speed and wind energy
Renewable Energy, 145 (2020), pp. 2373-2379.
Dong and Shi, 2019 Dong F.G., Shi L.
Regional differences study of renewable energy performance: A case of wind power in China
Journal of Cleaner Production, 233 (2019), pp. 490-500.
Duan et al., 2021 Duan J., Wang P., Ma W., Tian X., Fang S., Cheng Y., . . . Liu H.
Short-term wind power forecasting using the hybrid model of improved variational mode decomposition and Correntropy Long Short-term memory neural network
Energy, 214 (2021).
Dong et al., 2011 Dong L., Wang L., Hao Y., Hu G., Liao X.
PREDICTION OF WIND POWER GENERATION BASED ON AUTOREGRESSIVE MOVING AVERAGE MODEL
Acta Energiae Solaris Sinica, 32(2011), pp. 617-622.
Ding et al., 2019 Ding M., Zhou H., Xie H., Wu M., Nakanishi Y., Yokoyama R.
A gated recurrent unit neural networks based wind speed error correction model for short-term wind power forecasting
Neurocomputing, 365 (2019), pp. 54-61.
Diyaley et al., 2019 Diyaley, S., Biswas, AB., & Chakraborty, S.
Determination of the optimal drill path sequence using bat algorithm and analysis of its optimization performance
Journal of Industrial and Production Engineering, 36(2018), pp.97-112
Duran et al., 2007 Duran M.J., Cros D, Riquelme J.
Short-term wind power forecast based on ARX models
Journal of Energy Engineering-Asce, 133(2007), pp. 172-180.

Das et al., 2020 Das S., Sahu T. P., Janghel RR.
PSO-based group-oriented crow search algorithm (PGCSA)
Engineering Computations.

Engie, 2018. The La Haute Borne wind farm data set. https://opendata-renewables.engie.com/explore/?sort=modified

Eissa et al., 2018 Eissa M., Yu J.L., Wang S.Y., Peng L.
Assessment of Wind Power Prediction Using Hybrid Method and Comparison with Different Models
Journal of Electrical Engineering & Technology, 13(2018), pp. 1089-1098.

Foley et al., 2012 Foley A.M., Leahy P.G., Marvuglia A., McKeogh E.J.
Current methods and advances in forecasting of wind power generation
Renewable Energy, 37(2012), pp. 1-8.

Fu et al., 2019 Fu C., Li G.Q., Lin K.P., Zhang H.J.
Short-Term Wind Power Prediction Based on Improved Chicken Algorithm Optimization Support Vector Machine
Sustainability, 11(2019), 15.

Gupta et al., 2018 Gupta D., Sundaram S., Khanna A., Hassanien A.E., de Albuquerque V.H.C.,
Improved diagnosis of Parkinson's disease using optimized crow search algorithm
Computers & Electrical Engineering, 68 (2018), pp. 412-424.

Guermoui et al., 2018 Guermoui M., Melgani F., Danilo C.
Multi-step ahead forecasting of daily global and direct solar radiation: A review and case study of Ghardaia region
Journal of Cleaner Production, 201 (2018), pp. 716-734.

Habib et al., 2020 Habib A., Abbassi R., Aristizabal A.J., Abbassi A.
Forecasting model for wind power integrating least squares support vector machine, singular spectrum analysis, deep belief network, and locality-sensitive hashing
Wind Energy, 23(2020), pp. 235-257.

Huang et al., 2012 Huang G.B., Zhou H.M., Ding X.J., Zhang R.
Extreme Learning Machine for Regression and Multiclass Classification
IEEE Transactions on Systems Man and Cybernetics Part B-Cybernetics, 42(2012), PP. 513-529.

Huang et al., 2011 Huang G.B., Wang D.H., Lan Y.
Extreme learning machines: a survey
International Journal of Machine Learning and Cybernetics, 2(2011), PP. 107-122.

Huang et al., 2020 Huang Y., Li J., Hou W., Zhang B., Zhang Y., Li Y., Sun L.
Improved clustering and deep learning based short-term wind energy forecasting in large-scale wind farms
Journal of Renewable and Sustainable Energy, 12(2020).

Jacobson and Delucchi, 2011 Jacobson M.Z., Delucchi M.A
Providing all global energy with wind, water, and solar power, Part I: Technologies, energy resources, quantities and areas of infrastructure, and materials
Energy Policy, 39(2011), pp. 1154-1169.

Jiang et al., 2017 Jiang Y., Chen X.Y., Yu K., Liao Y.C.
Short-term wind power forecasting using hybrid method based on enhanced boosting

algorithm
Journal of Modern Power Systems and Clean Energy, 5(2017), pp. 126-133.
Jung and Broadwater, 2014., Jung J., Broadwater R.P.
Current status and future advances for wind speed and power forecasting
Renewable & Sustainable Energy Reviews, 31 (2014), pp. 762-777.
Karaboga and Basturk, 2007 Karaboga D., Basturk B.
A powerful and efficient algorithm for numerical function optimization: artificial bee colony (ABC) algorithm
Journal of Global Optimization, 39(2007), pp. 459-471.
Karakus et al., 2017 Karakus O., Kuruoglu E.E., Altinkaya M.A.
One-day ahead wind speed/power prediction based on polynomial autoregressive model
IET Renewable Power Generation, 11(2017), pp. 1430-1439.
Kamat, 2007 Kamat, P. V. 2007
Meeting the clean energy demand: Nanostructure architectures for solar energy conversion
Journal of Physical Chemistry C, 111(2007), pp. 2834-2860.
Korprasertsak and Leephakpreeda, 2019 Korprasertsak N., Leephakpreeda T.
Robust short-term prediction of wind power generation under uncertainty via statistical interpretation of multiple forecasting models
Energy, 180 (2019), pp. 387-397.
Liu et al., 2020 Liu BC, Zhao SJ, Yu XG, Zhang L, Wang QS.
A Novel Deep Learning Approach for Wind Power Forecasting Based on WD-LSTM Model
Energies, 13(2020), 17.
Liu et al., 2018 Liu B.Y., Wang G.S., Tseng M.L., Wu K.J., Li Z.G.
Exploring the reliable power module on the electro-thermal parameters : Insulated Gate Bipolar Transistor junction and case temperature
Energies, 11(2018), 2371.
Li et al., 2018 Li C.B., Lin S.S., Xu F.Q., Liu D., Liu J.C.
Short-term wind power prediction based on data mining technology and improved support vector machine method: A case study in Northwest China
Journal of Cleaner Production, 205(2018), pp. 909-922.
Li et al., 2020 Li L.L, Chang Y.B, Tseng M.L., Liu J.Q., Lim M.K.
Wind power prediction using a novel model on wavelet decomposition-support vector machines-improved atomic search algorithm
Journal of Cleaner Production, 270 (2020).
Li et al., 2020 Li L.L., Zhao X., Tseng M.L., Tan R.R.
Short-term wind power forecasting based on support vector machine with improved dragonfly algorithm
Journal of Cleaner Production, 242(2020), 12.
Lu et al., (2020) Lu X., Kanghong D., Guo L., Wang P., Yildizbasi A.
Optimal estimation of the Proton Exchange Membrane Fuel Cell model parameters based on extended version of Crow Search Algorithm
Journal of Cleaner Production, 272 (2020).

Liu et al., 2019 Liu Y., Guan L., Hou C., Han H., Liu Z.J., Sun Y., Zheng M.H.
Wind Power Short-Term Prediction Based on LSTM and Discrete Wavelet Transform
Applied Sciences-Basel, 9(2019), 17.

Lin et al., 2015 Lin Y.J., Kruger U., Zhang J.P., Wang Q., Lamont L., El Chaar L
Seasonal Analysis and Prediction of Wind Energy Using Random Forests and ARX Model Structures
IEEE Transactions on Control Systems Technology, 23(2015), pp. 1994-2002.

Liu et al., 2020 Liu Z.F., Li L.L., Tseng M.L., Lim M.K.
Prediction short-term photovoltaic power using improved chicken swarm optimizer - Extreme learning machine model
Journal of Cleaner Production, 248(2020), 14.

Ma et al., 2020 Ma J.Y., Yang M., Lin Y.
Ultra-Short-Term Probabilistic Wind Turbine Power Forecast Based on Empirical Dynamic Modeling
IEEE Transactions on Sustainable Energy, 11(2020), pp. 906-915.

Mirjalili, 2015 Mirjalili S., 2015
Moth-flame optimization algorithm: A novel nature-inspired heuristic paradigm
Knowledge-Based Systems, 89(2015), pp. 228-249.

Mirjalili, 2014 Mirjalili S., Mirjalili S.M., Lewis A
Grey Wolf Optimizer
Advances in Engineering Software, 69 (2014), pp. 46-61.

Nizar et al., 2008 Nizar A.H., Dong Z.Y., Wang Y.
Power utility nontechnical loss analysis with extreme learning machine method
IEEE Transactions on Power Systems, 23(2008), PP. 946-955.

Oliva et al., 2017 Oliva D., Hinojosa S., Cuevas E., Pajares G., Avalos O., Galvez J.
Cross entropy based thresholding for magnetic resonance brain images using Crow Search Algorithm
Expert Systems with Applications, 79(2017), pp. 164-180.

Papadopoulos, 2020 Papadopoulos A.M.
Renewable energies and storage in small insular systems: Potential, perspectives and a case study
Renewable Energy, 149 (2020), pp. 103-114.

Sayed et al., 2019 Sayed G.I., Hassanien A.E., Azar A.T.
Feature selection via a novel chaotic crow search algorithm
Neural Computing & Applications, 31(2019), pp. 171-188.

Shi et al., 2012 Shi J., Guo J.M., Zheng S.T. Evaluation of hybrid forecasting approaches for wind speed and power generation time series
Renewable & Sustainable Energy Reviews, 16(2012), pp. 3471-3480.

Song et al., 2018 Song J., Wang, J., Lu H.
A novel combined model based on advanced optimization algorithm for short-term wind speed forecasting
Applied Energy, 215 (2018), pp. 643-658

Suresh et al., 2010 Suresh S., Saraswathi S., Sundararajan N.
Performance enhancement of extreme learning machine for multi-category sparse data

classification problems
Engineering Applications of Artificial Intelligence, 23(2010), pp. 1149-1157.
Salcedo-Sanz et al., 2011 Salcedo-Sanz S., Ortiz-Garcia E. G., Perez-Bellido A.M., Portilla-Figueras A., Prieto L.
Short term wind speed prediction based on evolutionary support vector regression algorithms
Expert Systems with Applications, 38(2011), pp. 4052-4057.
Shekhawat and Saxena, 2020 Shekhawat S., Saxena, A.
Development and applications of an intelligent crow search algorithm based on opposition based learning
Isa Transactions, 99 (2020), pp. 210-230.
Tang et al., 2016 Tang J.X., Deng C.W., Huang G.B.
Extreme Learning Machine for Multilayer Perceptron
IEEE Transactions on Neural Networks and Learning Systems, 27(2016), PP. 809-821.
Tu et al., 2020 Tu C.S., Hong C.M., Huang H.S., Chen C.H.
Short Term Wind Power Prediction Based on Data Regression and Enhanced Support Vector Machine Energies, 13(2020).
Wang et al., 2020 Wang J.J., Liang Y.Y., Zheng Y.H., Gao R.X., Zhang F.L.
An integrated fault diagnosis and prognosis approach for predictive maintenance of wind turbine bearing with limited samples
Renewable Energy, 145 (2020), pp. 642-650.
Wolpert et al., 1997 Wolpert D.H. Macready W.G.
No free lunch theorems for optimization
IEEE Transactions on Evolutionary Computationvolume, 1 (1997), pp. 67–82.
Vargas et al., 2019 Vargas S.A., Esteves G.R.T., Macaira P.M., Bastos B.Q., Oliveira F.L.C., Souza R.C.
Wind power generation: A review and a research agenda
Journal of Cleaner Production, 218 (2019), pp. 850-870.
Xia et al., 2020 Xia J., Ma X., Wu W.Q., Huang B.L., Li W.P.
Application of a new information priority accumulated grey model with time power to predict short-term wind turbine capacity
Journal of Cleaner Production, 244 (2020), 20.
Yin et al., 2019 Yin H., Ou Z.H., Huang S.Q., Meng A.B.
A cascaded deep learning wind power prediction approach based on a two-layer of mode decomposition
Energy, 189(2019), 11.
Yuan et al., 2015 Yuan X.H., Chen C., Yuan Y.B., Huang Y.H., Tan Q.X.
Short-term wind power prediction based on LSSVM-GSA model
Energy Conversion and Management, 101 (2015), pp. 393-401.
Zhou et al., 2021 Zhou B., Duan H., Wu Q., Wang H., Or S.W., Chan K.W., Meng Y.
Short-term prediction of wind power and its ramp events based on semi-supervised generative adversarial network
International Journal of Electrical Power & Energy Systems, 125 (2021).
Zhang et al., 2019 Zhang G., Liu H.C., Zhang J.B., Yan Y., Zhang L., Wu C., . . . Wang Y.Q.

Wind power prediction based on variational mode decomposition multi-frequency combinations
Journal of Modern Power Systems and Clean Energy, 7(2019), pp. 281-288.

Zheng and Wu, 2019 Zheng H., Wu Y.H.
A XGBoost Model with Weather Similarity Analysis and Feature Engineering for Short-Term Wind Power Forecasting
Applied Sciences-Basel, 9(2019), 12.

Zhang et al., 2020 Zhang P., Wang Y.L., Liang L.K., Li, X., Duan Q.T.
Short-Term Wind Power Prediction Using GA-BP Neural Network Based on DBSCAN Algorithm Outlier Identification
Processes, 8(2020), 15.

Zhang et al., 2020 Zhang Y.G., Zhao Y., Kong C.H., Chen B.
A new prediction method based on VMD-PRBF-ARMA-E model considering wind speed characteristic
Energy Conversion and Management, 203 (2020), 18.